

The Surface Atomic Oxyradical Mechanism for Ag-Catalyzed Olefin Epoxidation¹

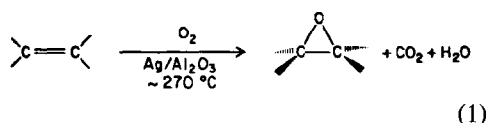
EMILY A. CARTER² AND WILLIAM A. GODDARD III³

*Arthur Amos Noyes Laboratory of Chemical Physics, California Institute of Technology,
Pasadena, California 91125*

Received October 15, 1987; revised January 25, 1988

We report comprehensive, quantitative, ab initio theoretical estimates for the energetics involved in the Ag-catalyzed epoxidation of olefins. From these estimates, a detailed mechanism is proposed. This mechanism (based on theoretical quantum chemical studies of the interaction of atomic and molecular adsorbates with clusters of Ag atoms) proposes that a *surface atomic oxyradical anion* is the active oxygen species for forming epoxide. This mechanism explains the role of electronegative (Cl^-) and electropositive (Cs^+) promoters and explains why selectivity (toward epoxide) is far higher for ethylene than for propene and other higher olefins. Recent experiments which suggested $\text{O}_{2(\text{ad})}$ as the active species are reinterpreted within the context of this new atomic oxygen radical mechanism. © 1988 Academic Press, Inc.

The heterogeneous selective oxidation of olefins to epoxides by promoted Ag is a several billion dollar a year industry, with the epoxides providing an entry into glycols, polymers, and other specialty chemicals. The process involves the interaction of the olefin with oxygen over an alumina-supported Ag catalyst at typical reaction temperatures of $\sim 270^\circ\text{C}$ and pressures of 1–10 atm, to produce the corresponding epoxide along with undesirable combustion products (CO_2 and H_2O) (1a),



Although the reaction in (1) appears to be extremely simple, the mechanistic details of epoxide formation have eluded definitive results. Grasp of the key mechanistic features may lead to intelligent catalyst design to increase the selectivity for formation of epoxide beyond the current yields of 80–

90%, which would have a significant economic impact on the glycol and other industries.

Unique features of the epoxidation catalysis are the following (1–3): (i) Ag is especially active, with other metals typically producing mostly combustion products; (ii) both electronegative (e.g., Cl^-) and electropositive (e.g., Cs^+) elements promote the reaction; and (iii) the process is selective only for C_2H_4 , with higher olefins producing primarily CO_2 and H_2O .

Mechanistic controversies center around the nature of the oxygen species which performs the selective chemistry (e.g., whether absorbed dioxygen, $\text{O}_{2(\text{ad})}$, or monatomic oxygen, $\text{O}_{(\text{ad})}$, is the active precursor (1–4) and why electronegative and electropositive elements both act to increase the selectivity toward epoxide (5).

From a series of quantum chemical calculations on finite Ag clusters interacting with a variety of adsorbates (6), we have calculated heats of formation (Table 1) of various relevant adsorbed intermediates likely to play a role in epoxidation catalysis. Using these heats of formation, we assess the thermodynamic feasibility of possi-

¹ Contribution No. 7647.

² Present address: Department of Chemistry, University of Colorado, Boulder, CO 80309.

³ To whom correspondence should be addressed.

TABLE I

Heats of Formation (at 298°K) of Adsorbed Species on Ag (kcal/mol)

Adsorbate	$\Delta H_{f,298}^\circ$
$O_{(ad)}$	-19
$O_{2(ad)}$	-10
$OH_{(ad)}$	-46
$C_2H_{4(ad)}$	+3
$C_2H_{4(g)}$	+12
$C_3H_{6(ad)}$	-4
$C_3H_{6(g)}$	+5
$-OCH_2\dot{C}H_{2(ad)}$	-12
$-OCH_2\dot{C}HCH_3_{(ad)}$	-22
$-OCH=CH_{2(ad)}$	-26
$-OCH=CHCH_3_{(ad)}$	-34
$-OCH_2CH=CH_{2(ad)}$	-32
$\underline{C}H_2CH_2\dot{O}_{(ad)}$	-23
$\dot{C}HCH_3CH_2\dot{O}_{(ad)}$	-32
$-OCH_2\dot{C}H_{(ad)}$	+51

ble pathways through which epoxidation and combustion may occur. These quantum chemical calculations result in a new candidate, the surface atomic oxyradical, for the active species responsible for oxidation. Previous experiments on Ag single crystals (5f, 7) and Ag powders (8) have led to conflicting interpretations regarding whether adsorbed O or O_2 is the active oxygen species for forming epoxide. We are able to give a comprehensive, consistent interpretation of these conflicting experiments in terms of a new epoxidation scheme: *the surface atomic oxyradical (SAO) mechanism*. The role of Cl and Cs, as representatives of the two classes of promoters, is also explained. New experiments are suggested to test various concepts of our postulated mechanism and keys to suppressing combustion (e.g., changing the reaction conditions) are discussed. The new mechanism, as outlined below, is more comprehensive and more detailed in its description of reaction pathways than previous mechanisms. Furthermore, this work offers the first quantitative thermodynamic estimates for each reaction step and, in addition, offers a detailed description of the electronic character of chemisorbed oxygen.

OXYGEN CHEMISORPTION

Figure 1 displays a qualitative potential energy surface for the interaction of $O_{2(g)}$ with a Ag surface. Since O_2 is known to adsorb dissociatively above 150–200°K on Ag (9), monatomic oxygen is the primary oxygen species present under typical reaction conditions ($T \sim 540^\circ\text{K}$). Experimentally, O_2 has a molecular chemisorption binding energy of ~ 10 kcal/mol (9, 10), with a small (< 10 kcal/mol) barrier to dissociation from the chemisorbed state. Since the coverage of O_2 is negligibly small under typical reaction conditions ($\theta_{O_2} = 1.21 \times 10^{-9}$ at 1 atm O_2 and $T = 540^\circ\text{K}$ (11a) and since we find that direct attack of $O_{2(ad)}$ on ethylene is subject to a barrier of ≥ 15 kcal/mol (at least 5 kcal/mol higher than the barrier to dissociation), we conclude that $O_{2(ad)}$ does not play a direct role in the catalysis (11b).

The nature of $O_{2(ad)}$ is predicted to resemble $O_{2(ad)}^-$ lying parallel to the surface (Fig. 1) (6). The vibrational frequency calculated for $O_{2(ad)}^-$ is ~ 1260 cm^{-1} , in good agreement with recent EELS data for O_2 adsorbed on polycrystalline silver [$\omega_e(\text{O}-\text{O}) \sim 1300$ cm^{-1}] (11c). The frequency of $O_{2(ad)}$ on Ag(110) is anomalously low ($\omega_e \sim 640$ cm^{-1}) (12a) and has often been ascribed to a O_2^{2-} species, a highly unstable dianion. A less severe view of $O_{2(ad)}$ on Ag(110) may be to consider it as a *cis*-dimetallaperoxide, in which the substituents are now much heavier than those in H_2O_2 , leading to a very low $\omega_e(\text{O}-\text{O})$.

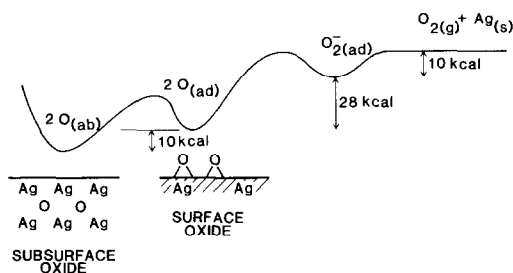
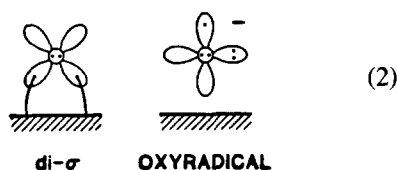


FIG. 1. Potential energy diagram for interaction of oxygen with Ag surface.

From Redhead analyses (*11d*) of the second-order desorption kinetics for $O_{(a)}$ on Ag(111) and two different coverages of $O_{(ad)}$ on Ag(110), we calculate identical binding energies for O/Ag(111) and the high-coverage state of O/Ag(110) [$D(\text{Ag-O}) = 76.6$ kcal/mol] and a slightly stronger binding energy for the low-coverage $O_{(a)}$ on Ag(110) [$D(\text{Ag-O}) = 78.1$ kcal/mol]. These values are in excellent agreement with our theoretical prediction of 78–79 kcal/mol for $O_{(ad)}$ on Ag (6). Thus the heat of dissociative chemisorption of dioxygen on Ag is ~ 38 kcal/mol (Fig. 1). Above $\sim 370^\circ\text{K}$, oxygen diffuses into the subsurface layers of Ag (*12a*). This subsurface oxide desorbs between 780 and 850°K , implying a binding energy of about 83 kcal/mol (Fig. 1) (*12a,e,f*).

Theoretical calculations of O adsorbed in the threefold site on Ag suggest the existence of two nearly degenerate states of oxygen with similar binding energies (79 versus 78 kcal/mol) but with very different character (6). The ground state oxyradical has an unpaired (radical) electron in a p orbital, perpendicular to the surface. In contrast, the di- σ oxide excited state (1 kcal/mol higher) has both electrons of O atom paired into bonds to the metal surface.



We predict very different properties for these two species, with the atomic oxyradical exhibiting a long perpendicular distance from the surface of 1.80 \AA [$R_e(\text{Ag-O}) = 2.45 \text{ \AA}$] and an Ag–O stretching frequency of 299 cm^{-1} , while the di- σ oxide is 1.37 \AA from the surface [$R_e(\text{Ag-O}) = 2.16 \text{ \AA}$] with $\omega_e(\text{Ag-O}) = 412 \text{ cm}^{-1}$. These values may be compared with the observed EEL spectrum (*12a*) for $O_{(ad)}$ on Ag(110), where the Ag–O vibration is found at 315 cm^{-1} and SEXAFS data (*12c*) [for the p -(2×1)-O overlayer

on Ag(110), where $\theta_0 = 0.5$] in which $R(\text{Ag-O}) = 2.06$ and 2.17 \AA for the nearest and next-nearest neighbor silver atoms, respectively. (The next-nearest neighbor Ag atoms are the second-layer Ag atoms which contribute to the four-coordinate trough site.) SEXAFS data are unavailable for the three-coordinate site on Ag(110) or Ag(111), which we suspect (*vide infra*) to be the oxyradical species, with a long $R(\text{Ag-O})$ and a lower Ag–O vibration. Consistent with the findings of Benndorf *et al.*, who observed a 220 cm^{-1} loss in the EELS for O/Ag(111) (*12d*), nearly 100 cm^{-1} lower than for O/Ag(110), we predict a similar lowering of the vibrational frequency for O/Ag(111) [$\omega_e = 299 \text{ cm}^{-1}$] versus O/Ag(110) [$\omega_e = 412 \text{ cm}^{-1}$].

The *surface atomic oxyradical* ground state of $O_{(ad)}$, with its unpaired electron in the orbital pointing away from the surface, should be quite reactive toward a variety of substrates (CO, olefins, etc.), whereas the di- σ oxide should be less reactive, since the electrons on oxygen are strongly coupled to the surface. In particular, because of its unpaired electron, the SAO state should attack the π -bond of an olefin to form the epoxide precursor (Fig. 2) with essentially no barrier. This precursor should have little or no energy barrier for closure to form epoxide, leading to a rapid, two-step process. Evidence for such a two-step process involving a primary carbon radical undergoing partial randomization of stereochemistry is provided by the labeling studies of Cant and Hall (*13a*), who found that either *cis*- or *trans*- d_2 ethylene produced a mixture of *cis*- and *trans*- d_2 epoxide which was 92% equilibrated.

As an experimental probe for the presence of the atomic oxyradical state, we suggest NEXAFS (near edge X-ray absorption fine structure). With an unpaired electron residing in an orbital perpendicular to the surface, the X-ray absorption should reach a minimum at normal incidence of polarized light and a maximum at grazing incidence (with the electric vector perpendicular to

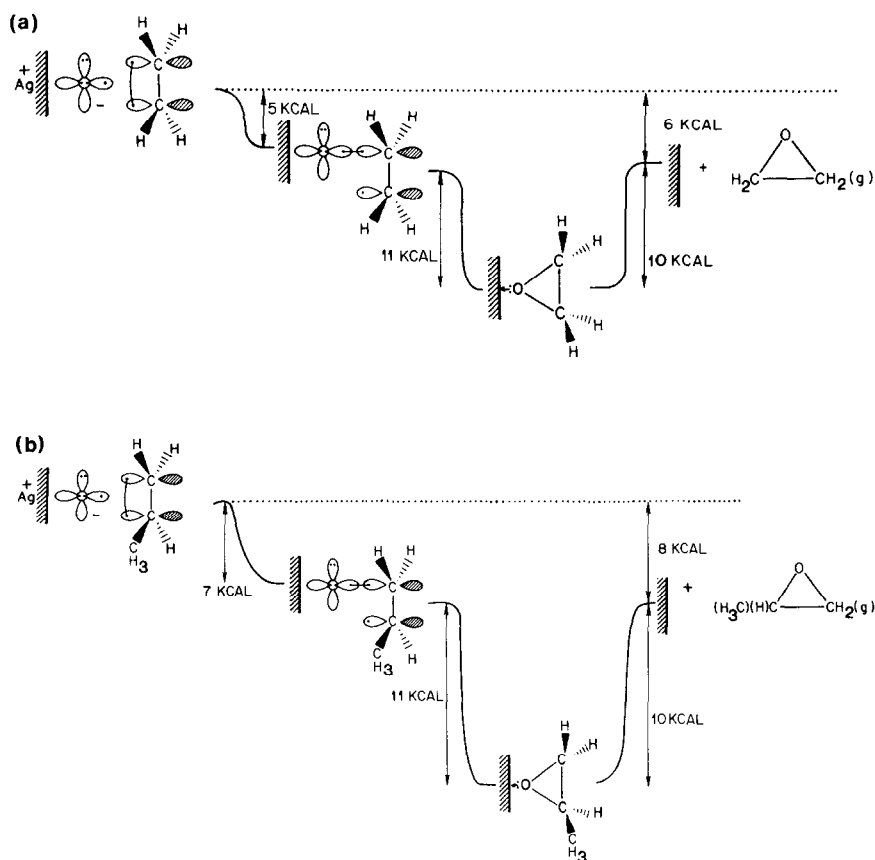


FIG. 2. Thermodynamics of epoxidation for ethylene (a) and propene (b).

the surface). Earlier studies (13b,c) probing for oxygen radicals using electron paramagnetic resonance (EPR) techniques were carried out on supported catalysts, where it is difficult to accurately assess the oxygen coverage. While Shimizu *et al.* (13b) did not report an estimate for θ_{O} , Clarkson and Cirillo (13c) determined θ_{O} to be ~ 0.44 for their catalyst. Since we predict the SAO to exist only above $\theta_{\text{O}} = 0.5$ and since we predict that the di- σ oxide (with no radical character) is preferred at $\theta_{\text{O}} < 0.5$ (vide infra), we do not expect an EPR signal for O^- to be present on these supported catalysts, consistent with the findings of these previous studies. In order to test the existence of atomic oxygen radicals with EPR, experiments with oxygen coverages above one-half a monolayer are required.

EPOXIDATION AND COMBUSTION ENERGETICS

Figure 2a displays the thermodynamics of epoxidation as expected from our cluster calculations for ethylene reacting with the surface atomic oxyradical. We find that each step leading to the formation of adsorbed epoxide is favorable, with the overall reaction downhill by 6 kcal/mol. [These energetics are based on a gas phase olefin interacting with the SAO (an Eley-Rideal mechanism). If the olefin is adsorbed when it interacts with $\text{O}_{(\text{ad})}$ (Langmuir-Hinshelwood), then the heat of adsorption of the olefin (which varies from ~ 5 to 10 kcal/mol depending on the coverage of oxygen) will push the energy of the reactants shown in Fig. 2 down by 5–10 kcal/mol, rendering the reaction nearly thermoneutral.] Analo-

gous radical addition processes in the gas phase are known to exhibit extremely low barriers (0–2 kcal/mol) (14a), and thus we expect small barriers for the steps in Fig. 2.

The SAO state is ideally posed for direct attack on the π -bond of the olefin, leading to an intermediate which would close selectively to form epoxide. The rate-determining step would be the reaction of SAO with gas phase or weakly adsorbed olefin. However, this cannot be the whole story, because the same energetics (see Fig. 2b) apply to propene (C_3H_6), whereas experimental epoxide yields are 40–90% for C_2H_4 (depending on the catalyst) but only 0–6% for propene (4, 14b,c). Thus, although thermodynamically and kinetically feasible, a competing pathway to combustion must be operative for propene, while this route must not be so accessible for ethylene.

The explanation that leaps to mind for the combustion propensity of propene is hydrogen abstraction by surface oxygen (to form allyl radical), followed by reaction of the resulting radicals with other surface ox-

ygens to form CO_2 and H_2O . Indeed, we find that abstraction of H from C_2H_4 by the surface atomic oxyradical to form $OH_{(ad)}$ and a vinyl radical is *uphill* by ~ 39 kcal/mol with an expected barrier of 44 kcal/mol (Fig. 3), whereas H abstraction from propene (to form allyl) is uphill by only ~ 9 kcal/mol with an expected barrier of 16 kcal/mol (Fig. 4). The contrast in abstraction energetics for the two olefins is due to the difference in the C–H bond strengths in C_2H_4 and C_3H_6 : 118 kcal/mol (15) for C_2H_4 and 88 kcal/mol (16) for C_3H_6 . (Primary H abstraction from propene results in the formation of a resonance-stabilized allyl radical.) Thus H abstraction from the reactant olefin is highly *unfavorable* for C_2H_4 (leading to small yields of CO_2), but is somewhat *favorable* for C_3H_6 , favoring combustion for propene. An experimental test of this direct H abstraction pathway would be to replace all allylic H's with other alkyl groups, e.g., *t*-butylethylene or styrene, to see if higher yields of epoxide are obtained.

Although attractive, the above explana-

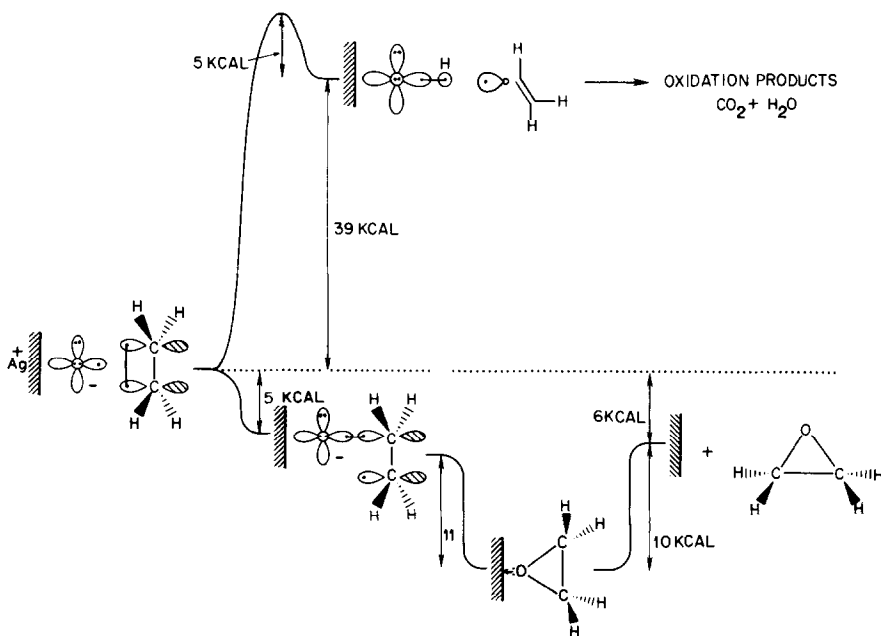


FIG. 3. Potential energy surface for the selective oxidation of ethylene to epoxide and for an initial step toward combustion (via H-atom abstraction from C_2H_4).

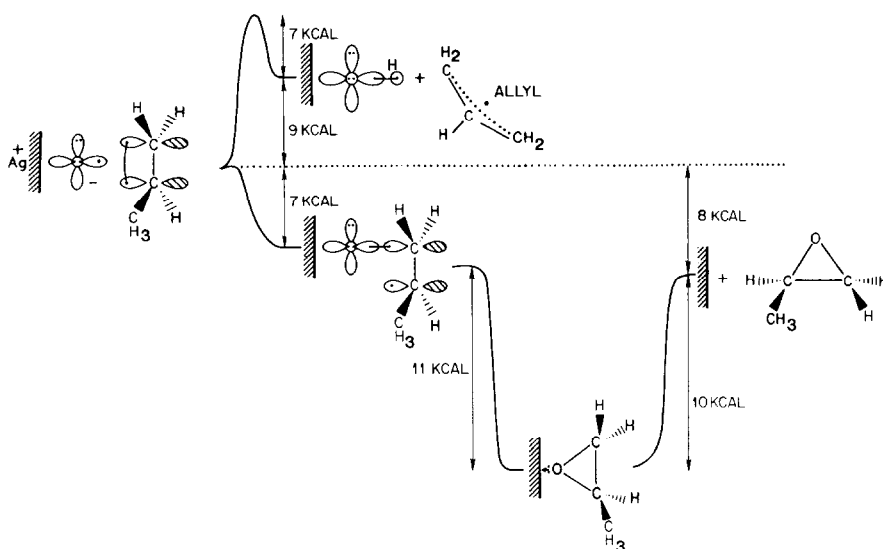


FIG. 4. Potential energy surface for the selective oxidation of propene to epoxide and for an initial step toward combustion (via H-atom abstraction from C_3H_6).

tion cannot be a complete one. We expect that formation of epoxide from propylene involves little or no barrier, whereas the H abstraction step (above) is endothermic by ~ 9 kcal/mol. Thus, of these two postulated pathways, the formation of propylene oxide should be favored thermodynamically and kinetically over direct hydrogen abstraction. Therefore allylic hydrogen abstraction from propene is not likely to be the primary combustion pathway.

Instead we propose that combustion of propene proceeds via the alternative route proposed in Fig. 5, where *after* the surface atomic oxyradical attacks the olefinic π -bond, a nearby surface oxygen abstracts the γ -H from the oxypropenyl radical to form $OH_{(ad)}$ and an adsorbed allyl alkoxy species (a process that is downhill by 37 kcal/mol!). Thus, after the oxypropenyl radical is formed ($\Delta H = -7$ kcal/mol), it may either

(i) close to form propylene oxide ($\Delta H = -11$ kcal/mol) or

(ii) react with a nearby surface oxygen ($\Delta H = -37$ kcal/mol) to form adsorbed allyl alkoxy (Fig. 6).

The large exothermicity of process (ii) suggests a very small barrier, due to early formation of a new π -bond upon γ -H abstraction. The combustion of propene may then continue via combustion of this allyl alkoxy intermediate. The initial step for this combustion pathway requires sufficient oxygen coverage such that oxygens are present in next-nearest neighbor (*nnn*) sites.

This two-step oxygen addition/ γ -H abstraction pathway for olefin combustion (we denote it as the OA/ γ H pathway) exhibits small barriers at each step and predicts the presence of a common intermediate (the oxyalkyl radical) en route to *both* epoxide and combustion products. Since the SAO mechanism suggests that the initial attack of olefin on SAO is rate-determining, the rates of combustion and selective oxidation should follow similar trends. For propene, combustion competes effectively with epoxidation because the γ -H's extend ~ 2.7 Å across the surface, within striking distance of a *nnn* $O_{(ad)}$ (2.9 Å away from the oxygen in the adsorbed oxypropenyl radical). On the other hand, such pathways are inaccessible for ethylene, since C_2H_4 has no γ -H's). Abstraction of a

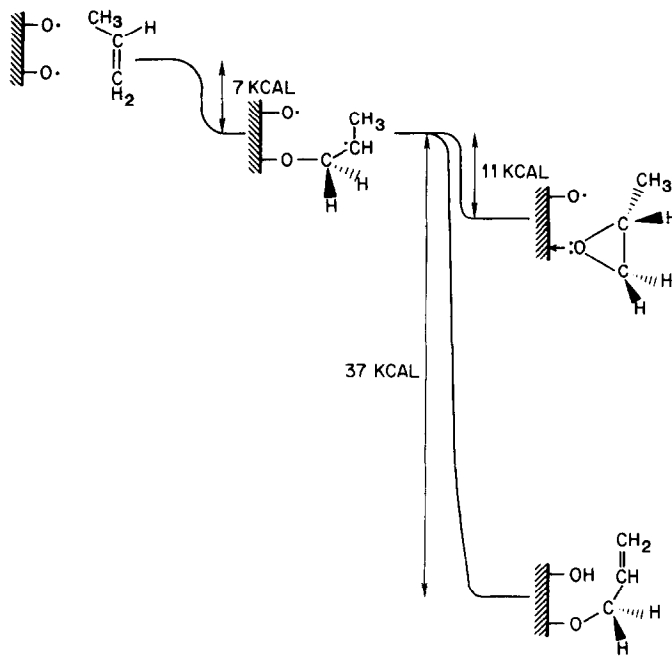


FIG. 5. Thermodynamics of combustion and epoxidation of propene via the oxygen addition common intermediate.

β -H is also unfavorable for both ethylene and propene, since an unstable carbene would be formed ($\Delta H = +36$ kcal/mol for ethylene). Abstraction of the α -H would be favorable for both ethylene and propene

($\Delta H_{\text{rxn}} = -41$ and -39 kcal/mol for ethylene and propene, respectively) but it is unlikely that this H can be close enough to a second surface oxyradical.

The formation of a common intermediate

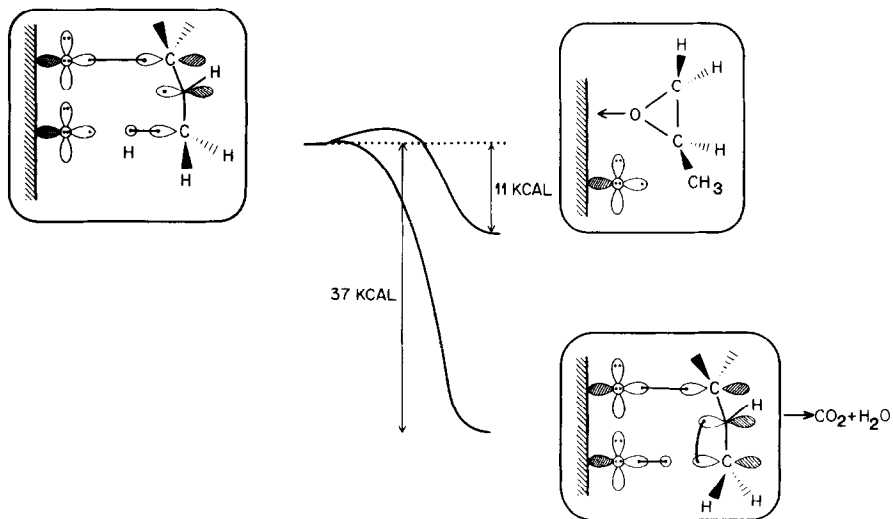


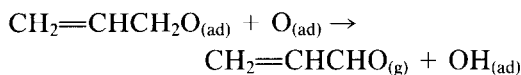
FIG. 6. Competing pathways for forming either adsorbed propylene oxide or the combustion precursor of propene from the oxypropenyl intermediate.

in the rate-determining step to both epoxide and $\text{CO}_2 + \text{H}_2\text{O}$ has also been suggested by Cant and Hall (13) and by Campbell (7a, 17) both of whom found that production of epoxide and combustion follow similar kinetics.

In order to test this mechanistic pathway, we suggest three experiments. The first is to follow the reaction of propene with $\text{O}/\text{Ag}(111)$ as a function of atomic oxygen coverage (θ_{O}). In the limit of very low coverages of $\text{O}_{(\text{ad})}$, our model predicts that selectivity to epoxide should increase due to the decrease in *nnn* oxygen adatoms necessary for combustion of the oxypropenyl intermediate. (Low coverages of $\text{O}/\text{Ag}(110)$ will not serve as an adequate test, since the di- σ oxide should prevail under these conditions, leading to only combustion products.) The second experiment is to expose allyl alcohol to an oxygen-precovered Ag surface. The dissociative adsorption of $\text{CH}_2=\text{CHCH}_2\text{OH}$ to form $\text{CH}_2=\text{CH}-\text{CH}_2\text{O}_{(\text{ad})} + \text{OH}_{(\text{ad})}$ is expected to be downhill by ~ 29 kcal/mol. The observation of combustion of $\text{CH}_2=\text{CHCH}_2\text{O}_{(\text{ad})}$ would be consistent with our mechanism, whereas if $\text{CH}_2=\text{CHCH}_2\text{O}_{(\text{ad})}$ does not combust in the presence of $\text{O}_{(\text{ad})}$, then our proposed mechanism for propene combustion is incomplete. In a third experiment, the allylic or γ -H positions of the olefin should be blocked using *t*-butylethylene or styrene. Our mechanism predicts that selectivity would increase. Although this last experiment does not distinguish between the two combustion pathways presented (H abstraction from the free olefin or from the adsorbed oxypropenyl radical), an unchanged combustion product yield would indicate that H abstraction from the allylic or γ position is not involved in the dominant combustion pathway.

Previous work by Geenen et al. (14b) indicated that the oxidation of propene over a Ag-Au alloy produced acrolein as the primary product. Allyl intermediates, although not directly observed, were proposed to explain the synthesis of acrolein.

Note that acrolein may be obtained within our mechanism as a subsequent oxidation product, obtained by α -H abstraction from adsorbed allyl alkoxide. Indeed, we estimate that the reaction



is exothermic by ~ 9 kcal/mol.

INTERPRETATION OF CONFLICTING EPOXIDATION EXPERIMENTS

Ag single-crystal studies by Campbell and co-workers (5, 7) have suggested that the steady-state coverage of monatomic oxygen is uncorrelated to the specific activity of the catalyst. Campbell measured the relative saturation coverages of $\text{O}_{(\text{ad})}$ on Ag(111) and Ag(110) and found them to differ by a factor of 18 [with a lower saturation coverage on Ag(111)] (7c). Since the activity on both surfaces only differed by a factor of ~ 2 [with Ag(110) exhibiting the greater activity], he concluded that monatomic oxygen plays no role in the reaction kinetics and suggested instead that $\text{O}_{2(\text{ad})}$ is responsible for epoxide formation. In addition, Campbell and Koel found that the postreaction oxygen coverage decreased substantially with increasing chlorine coverage, while the selectivity of the Ag catalyst in the presence of added Cl remained fairly constant (5b). The interpretation offered by these authors dismissed $\text{O}_{(\text{ad})}$ as the active epoxidation reagent and proposed $\text{O}_{2(\text{ad})}$ instead. However, no *direct evidence* for O_2 interacting with ethylene to form epoxide has been presented.

We suggest an alternative explanation of the experiments of Campbell and Koel which is consistent with our mechanism. Two high-symmetry adsorption sites exist on the corrugated (110) surface (Fig. 7):

- (a) a four-coordinate site in the trough involving two second-layer atoms and two first-layer atoms and
- (b) a three-coordinate site along the side

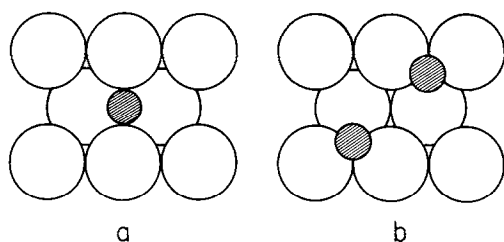


FIG. 7. The two high-symmetry adsorption sites for O on Ag(110): (a) the four-coordinate trough site (suitable for di- σ oxide) and (b) the three-coordinate site on the side of the trough (suitable for SAO).

of the trough (or a two-coordinate site at the crest).

We believe that the four-coordinate site leads to stronger bonding and to a di- σ -like oxide which is not as active as the oxyradical state favored at the lower-coordination site. This is consistent with LEED data from Menzel and co-workers (18) indicating that the four-coordinate trough sites fill first, resulting in a series of n by 1 patterns ($n = 2$ to 7), and with thermal desorption data of Campbell (19), who finds a peak temperature of 617°K (for $\theta_0 \leq 0.5$), in contrast to 579°K on Ag(111) (10). The maximum coverage for this site is $\theta_0 = 0.5$, exhibiting a p -(2 \times 1) LEED pattern. Campbell has shown that this species is relatively unreactive to CO (19). However, he has also observed a higher-coverage species which forms a c -(6 \times 2) overlayer, desorbs at a lower temperature (565°K), and is found to react five times more readily with CO to form CO₂ (19). We believe that this is the oxyradical state at the low-coordination site. On the other hand, the Ag(111) surface has only three-coordinate sites which we believe lead to the selective formation of oxyradical species, thus explaining the higher specific activity per surface site for Ag(111). The saturation coverage of oxygen is larger on the (110) surface than on the (111) surface, since *two* sites may be filled on the (110) plane whereas only *one* site may be used on the (111) [ignoring the small difference in properties expected for the fcc and hcp sites on the (111) surface]. Thus the

saturation coverage is greater on the (110) plane due to the accessibility of two kinds of sites rather than only one.

To test the proposed existence of two different types of oxygen adatoms, we suggest both NEXAFS and titration experiments. NEXAFS can probe for the presence of an unpaired electron on the adsorbate, as well as determine its relative orientation (e.g., the singly occupied p -orbital in the oxyradical, which should be perpendicular to the local surface). Titrating O_(ad), for instance, with CO₂ or NO₂, followed by exposure of the surface to ethylene, may reveal which type of oxygen is the precursor to epoxide. For example, we would expect the oxyradical species to react faster with NO₂ than with CO₂, reducing the yield of epoxide.

Supporting evidence for the role of adsorbed oxygen atoms in epoxidation comes from recent labeling studies by van Santen and de Groot (8a). Adsorption of ¹⁶O₂ at temperatures above 150–200°K resulted in an ¹⁶O atom-precovered surface. When these workers exposed an ¹⁶O-precovered Ag powder to a gaseous mixture of C₂H₄ and ¹⁸O₂, the initial product at early conversion was exclusively ¹⁶O-ethylene oxide. Unless the oxygen adatoms recombine immediately prior to reaction with ethylene, these experiments provide direct evidence that the epoxide is formed by reaction of the olefin with adsorbed monatomic oxygen. While other workers such as Twigg (20), Hayes (21), Force and Bell (22), Backx *et al.* (12a,b, 23), Grant and Lambert (7d,e), and van Santen and Kuipers (1a) have also suggested monatomic oxygen as the active epoxidation agent, there has not previously been a prediction of the microscopic nature of O_(ad), with a detailed prediction for electronic character of oxygen at high (SAO) and low (di- σ oxide) oxygen coverages.

We propose that catalyst activity may be controlled by maximizing the concentration of surface atomic oxyradical species present on the surface. This can be accomplished by saturating the surface so as to fill up the inactive (fourfold hollow) sites or by

stabilizing the SAO state. This idea that an active catalyst requires oxygen saturation is consistent with the experimental results on Ag powders where it is found that production of epoxide requires oxygen coverages higher than a 1 : 2 O : Ag ratio (8b).

THE ROLE OF PROMOTERS

Campbell and Koel have suggested that the effect of Cl is due to site-blocking (5b). This is based on the observation that as the coverage of Cl increases, less CO₂ is formed. They argue that the rate-determining steps in the combustion of C₂H₄ require a number of contiguous sites on the surface, whereas epoxidation may occur with a smaller, bare surface area. We agree that Cl acts as a site-blocker, but in our mechanism *it is the specific type of sites blocked by Cl which increase the selectivity*. This is consistent with the lack of any obvious trend in activity with Cl exposure. (The activity may increase or decrease upon addition of Cl under varying reaction conditions (5b, 17).) Our interpretation of Campbell and Koel's experiments is that Cl fills the four-coordinate trough sites, forcing the (di- σ bonded) oxygen adatoms out of the unreactive trough sites and into the reactive SAO state. Indeed, angle-resolved SIMS data of Winograd and co-workers (24) show that the height of Cl above the surface drops dramatically as the coverage of Cl on Ag(110) increases, which they interpret as Cl falling into the troughs of the (110) surface.

From coadsorption studies of cesium and oxygen on Ag(111), Campbell has shown that aggregates of approximate stoichiometry CsO₃ are formed under epoxidation reaction conditions (5d). Campbell suggests that the observed increase in selectivity is due to the same ensemble effect he proposed for Cl. We postulate an alternative interpretation in which Cs⁺ (atop three O_(ad)) acts as a strong Lewis acid and enhances the probability of adsorption of the olefin through a Lewis acid-Lewis base interaction. The selectivity is increased since

the best Lewis acid-Lewis base interaction involves maximal donation from the olefin π -bond. Maximum bonding involves holding the olefin parallel to the surface, making its π -bond readily accessible for attack by the SAO to form epoxide, and making the C-H bonds less accessible to abstraction (which would lead to combustion). Activity may increase due to the enhanced olefin sticking probability, but it also may decrease if Cs⁺ forms complexes with the surface atomic oxyradical species.

MECHANISTIC IMPLICATIONS FOR MAXIMUM SELECTIVITY

A common view of the mechanism for this reaction considers that adsorbed diatomic oxygen acts as the active precursor to epoxide (1). The model involves oxygen bound as a peroxyradical species, with one end up toward vacuum and one end σ -bonded to the surface, and assumes that the outer oxygen reacts with high selectivity to form epoxide. This leaves behind an adsorbed oxygen atom, which is presumed to react only in processes involved in combustion. This mechanism predicts a maximum selectivity for the formation of ethylene oxide of 6/7 or 85.7%. On the other hand, the surface atomic oxyradical mechanism has no implied limit on selectivity. Thus to increase the selectivity toward 100%, the challenge is to find ways to keep O_(ad) in the SAO state, by poisoning sites leading to other O_(ad) states. In particular, for Ag(110) we suggest that it is crucial to keep the oxygen surface coverage above one-half of a monolayer, in order to ensure production of the SAO. This is consistent with the enhanced reactivity found by Campbell above $\theta_{\text{O}} = 0.5$ and with van Santen and de Groot's observation that successful epoxidation requires oxygen to silver ratios above 1 : 2.

SUMMARY

Our current model of the mechanistic details of the Ag-catalyzed epoxidation reaction is as follows:

(i) The special activity of Ag relative to other transition metals is due to the fact that the olefin and its initial dissociation products are bound very weakly on the noble metals, whereas Group VIII metals bind olefins so strongly that they decompose rapidly to form $C_{(ad)} + H_{(ad)}$. While ethylene binds weakly to Cu, Ag, and Au, the unique quality about Ag relative to Cu and Au is that the oxygen adatoms can be formed readily (a large barrier to dissociative adsorption of O_2 exists on Au (25)) and that these $O_{(ad)}$ are sufficiently weakly bound O that epoxidation is favorable. (O on Cu readily forms an oxide of composition $Cu_{2.2}O$, where the oxygens are too strongly bound to react with olefins (26).)

(ii) The surface atomic oxyradical species is the active oxygen precursor to epoxide.

(iii) The pathways for the surface atomic oxyradical to convert olefin to epoxide are thermodynamically favorable with small barriers.

(iv) Combustion is favorable for higher olefins because of the presence of γ -H's accessible to oxyradicals in next-nearest neighbor surface sites. We propose the two-step oxygen addition/ γ -H abstraction mechanism as the most likely pathway for combustion. The reaction to form the allyl alkoxy intermediate is downhill by 37 kcal/mol, due to the formation of the new π -bond. Ethylene does *not* combust via the same pathway, since there are no γ -hydrogens, resulting in a high selectivity for epoxidation.

(v) The role of electronegative promoters is to block inactive sites for surface oxygen and to promote formation of the surface atomic oxyradical species.

(vi) The role of alkali promoters is to enhance olefin adsorption. In addition, the alkali metal cation holds the olefin parallel to the surface through a Lewis acid-Lewis base interaction, making the π -bond more accessible to the surface atomic oxyradical species and making the C-H bonds less accessible to reactions that may lead to combustion.

In summary, the surface atomic oxyradical mechanism explains the uniqueness of Ag, the selectivity for ethylene, the combustion of higher olefins, and the role of promoters. Experiments have been suggested to test various aspects of the proposed mechanism. This work reports the *first comprehensive* theoretical estimates for the energetics of explicit reaction pathways relevant in Ag-catalyzed olefin epoxidation.

ACKNOWLEDGMENTS

This work was initiated and continued with support by the Shell Development Corp. (1982-1985) and the Shell Companies Foundation (1985-1987). We particularly thank Drs. Charles Adams, Rutger van Santen, and John Cole for their roles in initiating and continuing this industrial support for our research. In addition, the work was partially funded by the National Science Foundation [Grant DMR82-15650 (1983-1986) and Grant CHE83-18041 (1986-1987)]. EAC acknowledges a National Science Foundation Predoctoral Fellowship (1982-1985), a research grant award from the International Precious Metals Institute and Gemini Industries (1985-1986), and a SOHIO Fellowship in Catalysis (1986-1987). We also thank Professors C. T. Campbell and B. E. Koel for useful discussions.

REFERENCES

1. (a) For a recent review, see van Santen, R. A., and Kuipers, H. P. C. E., "Advances in Catalysis," Vol. 35, p. 265. Academic Press, New York, 1987; (b) a classic review may be found in Voge, H. H., and Adams, C. R., "Advances in Catalysis" (D. D. Eley, P. W. Selwood, and P. B. Weisz, Eds.), Vol. 17, p. 151. Academic Press, New York, 1967.
2. Verykios, X. E., Stein, F. P., and Conghlin, R. W., *Catal. Rev. Sci. Eng.* **22**, 197 (1980).
3. Sachtler, W. M. H., Backx, C., and van Santen, R. A., *Catal. Rev. Sci. Eng.* **23**, 127 (1981).
4. Barteau, M., and Madix, R. J., in "The Chemical Physics of Solid Surfaces and Heterogeneous Catalysis" (D. A. King and D. P. Woodruff, Eds.), Vol. 4, Chap. 4. Elsevier, Amsterdam, 1982.
5. (a) Campbell, C. T., and Paffett, M. T., *Appl. Surf. Sci.* **19**, 28 (1984); (b) Campbell, C. T., and Koel, B. E., *J. Catal.* **92**, 272 (1985); (c) Campbell, C. T., *J. Catal.* **99**, 28 (1986); (d) Campbell, C. T., *J. Phys. Chem.* **89**, 5789 (1985); (e) Campbell, C. T., and Daube, K. A., *Surf. Sci.*, in press; (f) Campbell, C. T., in "Catalyst Characterization Science" (M. L. Deviney and J. L. Gland, Eds.), Vol. 288, p. 210. American Chemical Society Symp. Ser., Washington, DC, 1985; (g) Grant, R.

- B., and Lambert, R. M., *J. Catal.* **93**, 92 (1985); (h) Grant, R. B., and Lambert, R. M., *Langmuir* **1**, 29 (1985).
6. (a) Goddard, W. A. III, Low, J. J., Olafson, B. D., Redondo, A., Zeiri, Y., Steigerwald, M. L., Carter, E. A., Allison, J. N., and Chang, R., in "Proc. of the Symposium on the Chemistry and Physics of Electrocatalysis" (J. D. E. McIntyre, M. J. Weaver, and E. B. Yeager, Eds.), Vol. 84-12, pp. 63-95. The Electrochemical Society, Inc., Pennington, NJ, 1984; (b) Carter, E. A., and Goddard, W. A. III, submitted for publication.
 7. (a) Campbell, C. T., and Paffett, M. T., *Surf. Sci.* **139**, 396 (1984); (b) Campbell, C. T., *J. Vac. Sci. Technol. A* **2**, 1024 (1984); (c) Campbell, C. T., *J. Catal.* **94**, 436 (1985); (d) Grant, R. B., and Lambert, R. M., *J. Chem. Soc. Chem. Commun.*, 662 (1983); (e) *J. Catal.* **92**, 364 (1985).
 8. Van Santen, R. A., and de Groot, C. P. M., *J. Catal.* **98**, 530 (1986).
 9. Barteau, M. A., and Madix, R. J., *Surf. Sci.* **97**, 101 (1980).
 10. Campbell, C. T., *Surf. Sci.* **157**, 43 (1985).
 11. (a) A simple calculation using a steady-state expression for θ_{O_2} at 1 atm $O_{2(g)}$ and 540°K suggests

$$\theta_{O_2} = \frac{S_0^0 f_c}{\eta_s k_d} = 1.21 \times 10^{-9},$$

while θ_0 is surely greater than 0.5. S^0 , the initial sticking probability, is given an upper bound by the value reported by Campbell (10) of 5×10^{-6} at 147°K on clean Ag(111). (Surely at 540°K, S^0 will be much smaller due to the repulsive interactions with $O_{(ad)}$.) f_c , the flux of O_2 molecules impinging on the surface (at 760 Torr O_2 with $T = 540^\circ\text{K}$), is 2.04×10^{23} molec/cm²-sec. η_s on Ag(111) is 1.38×10^{15} sites/cm². k_d was calculated assuming a binding energy of 3 kcal/mol for O_2 on O/Ag(111) [the O_2 /Ag(111) physisorption binding energy (10) provides an upper bound due to O_2 -O repulsive interactions] and assuming a preexponential factor for first-order desorption of 10^{13} sec⁻¹. (b) The value of 14.6 kcal/mol is derived from gas-phase thermochemistry of $O_2^- + C_2H_4 \rightarrow ^-O_2CH_2CH_2^-$ and assumes an Eley-Rideal mechanism [$\Delta H_f(O_{2(g)}^-) = -10.1$ kcal/mol, $\Delta H_f(C_2H_{4(g)}) = 12.1$ kcal/mol, and $\Delta H_f(^-O_2CH_2CH_2^-) = 16.6$ kcal/mol, using values from Ref. (16)]. The barrier would be even higher if ethylene is adsorbed on the Ag surface. The barrier for addition of O_2^- to C_2H_4 may be alternatively estimated as follows. The reaction of O_2^- with C_2H_4 to form $^-O_2CH_2CH_2^-$ requires localization of an oxygen 2p electron previously delocalized in an $O_2 \pi_g$ orbital. This localization costs ~14 kcal/mol. [Estimated from the relative O-H bond strengths in H_2O_2 versus CH_3OH (HO_2^- loses the same delocalization as O_2^- whereas CH_3O^- does not). Thus $\Delta D_{298}(O-H) = D_{298}(CH_3O-H) -$

- $D_{298}(HO_2-H) = 13.9$ kcal/mol (16).] After localization of the O p orbital, radical addition to the π -bond of ethylene to form a C-O bond typically suffers a barrier of 0-2 kcal/mol. Therefore we estimate, independently, that $E_a \sim 14-16$ kcal/mol for the addition of O_2^- to C_2H_4 . This mechanism assumes that the C_2H_4 and O_2 are oriented for the best overlap between the C 2p and O 2p orbitals used to form the C-O bond, leading to a preferred parallel orientation of O_2 and C_2H_4 with respect to the surface. Thus we expect little change in the interaction of O_2 with Ag after formation of $^-O_2CH_2CH_2^-$. (c) Prabhakaran, K., and Rao, C. N. R., *Surf. Sci.* **186**, L575 (1987); (d) Redhead, P. A., *Vacuum* **12**, 203 (1962).
12. (a) Backx, C., de Groot, C. P. M., and Biloen, P., *Surf. Sci.* **104**, 300 (1981); (b) **115**, 382 (1982); (c) Puschmann, A., and Haase, J., *Surf. Sci.* **144**, 559 (1984); (d) Benndorf, C., Franck, M., and Thieme, F., *Surf. Sci.* **128**, 417 (1983); (e) Roviada, G., Pratesi, F., Maglietta, M., and Ferroni, E., *Surf. Sci.* **43**, 230 (1974); (f) Tan, S. A., Grant, R. B., and Lambert, R. M., *J. Catal.* **100**, 383 (1986).
 13. (a) Cant, N. W., and Hall, W. K., *J. Catal.* **52**, 81 (1978); (b) Shimizu, N., Shimokoshi, K., and Yasumori, I., *Bull. Chem. Soc. Japan* **46**, 2929 (1973); (c) Clarkson, R. B., and Cirillo, A. C., Jr., *J. Catal.* **33**, 392 (1974).
 14. (a) Westley, F., "Table of Recommended Rate Constants for Chemical Reactions Occurring in Combustion," NSRDS-NBS, p. 67. 1980; (b) Geenen, P. V., Boss, H. J., and Pott, G. T., *J. Catal.* **77**, 499 (1982); (c) Barteau, M. A., and Madix, R. J., *J. Amer. Chem. Soc.* **105**, 44 (1983).
 15. $\Delta H_{rxn} = +39.1$ kcal/mol for hydrogen abstraction from ethylene is derived from $D_{298}^0(C_2H_3-H) = 118.2$ kcal/mol [obtained by correcting D_0^0 by 1.5 kcal/mol ($\frac{3}{2}RT$) for finite temperature, where $D_0^0 = 116.7 \pm 1.2$ kcal/mol is from Shiromaru, H., Achiba, Y., Kimura, K., and Lee, Y. T., *J. Phys. Chem.* **91**, 17 (1987)], and the theoretically predicted binding energies of OH and O to the Ag surface (55 and 79 kcal/mol).
 16. Derived from "JANAF Thermochemical Tables," *J. Phys. Chem. Ref. Data* **14**, Suppl. 1 (1985) and from Benson, S. W., "Thermochemical Kinetics." Wiley, New York, 1976. The electron affinity for $^-O_2CH_2CH_2^-$ was approximated by the electron affinity of HO_2^- [$EA(HO_2^-) = 1.19$ eV] from Bierbaum, V. M., Schmitt, R. J., and DePuy, C. H., *J. Amer. Chem. Soc.* **103**, 6262 (1981).
 17. Other kinetic studies indicating similar rates for EO and CO₂ formation may be found in Ref. (5f).
 18. (a) Bradshaw, A. M., Engelhardt, H. A., and Menzel, D., *Ber. Bunsenges. Phys. Chem.* **76**, 501 (1972); (b) Engelhardt, H. A., and Menzel, D., *Surf. Sci.* **40**, 140 (1973); (c) Heiland, W., Iberl,

- F., Taglauer, E., and Menzel, D., *Surf. Sci.* **53**, 383 (1975); (d) Engelhardt, H. A., and Menzel, D., *Surf. Sci.* **57**, 591 (1976); (e) Engelhardt, H. A., Bradshaw, A. M., and Menzel, D., *Surf. Sci.* **40**, 410 (1973).
19. Campbell, C. T., and Paffett, M. T., *Surf. Sci.* **143**, 517 (1984).
20. Twigg, G. H., *Trans. Faraday Soc.* **42**, 284 (1946); *Proc. R. Soc. London Ser. A* **188**, 92 (1946).
21. Hayes, K. E., *Canad. J. Chem.* **38**, 2256 (1960).
22. Force, E. L., and Bell, A. T., *J. Catal.* **38**, 440 (1975); **40**, 356 (1975).
23. Backx, C., Moolhuysen, J., Geenen, P., and van Santen, R. A., *J. Catal.* **72**, 364 (1981).
24. Moon, D. W., Bleiler, R. J., and Winograd, N., *J. Chem. Phys.* **85**, 1097 (1986).
25. Sault, A., Madix, R. J., and Campbell, C. T., *Surf. Sci.* **169**, 347 (1986).
26. Inui, T., Ueda, T., and Suehiro, M., *J. Catal.* **65**, 166 (1980).